Available online at www.sciencedirect.com
SCIENCE DIRECT®
Optics Communications 224 (2003) 221–227
OPTICS COMMUNICATIONS
www.elsevier.com/locate/optcom

Isotropic *n*-dimensional fringe pattern normalization

Juan Antonio Quiroga[a,*], Manuel Servin[b,1]

[a] *Departamento de Óptica, Facultad de Ciencias Físicas, Universidad Complutense, Ciudad Universitaria s/n, Madrid 28040, Spain*
[b] *Centro de Investigaciones en Optica AC, PO Box 1-948, Leon Gto 37150, Mexico*

Received 7 April 2003; received in revised form 17 July 2003; accepted 30 July 2003

Abstract

Fringe pattern normalization consists in the background suppression and modulation normalization of a given fringe pattern, this process gives as a result a pure sinusoidal phase modulated signal. Normalization is an important operation in the demodulation of the phase from a single fringe pattern where spatially varying background and/or modulation act as error sources. The solution proposed is a direct and isotropic operator, based on the application of an *n*-dimensional quadrature transform. We have applied the method to simulated as well as experimental data with good results.

1. Introduction

In the first approximation it is possible to model the irradiance distribution of a given fringe pattern as an *n*-dimensional phase modulated signal given by

$$I(\mathbf{r}) = b(\mathbf{r}) + m(\mathbf{r})\cos\phi(\mathbf{r}), \tag{1}$$

where I is the irradiance, b the background, m the modulation, ϕ the modulating phase and $\mathbf{r} = (x_1, \ldots, x_n)$ denotes an n-dimensional position vector (for example, in a temporal experiment where a series of images are obtained $n = 3$ and $\mathbf{r} = \mathbf{r}(x, y, t)$ being t the time and x, y the spatial coordinates). Usually, in this model the modulating phase is associated to the physical magnitude to be measured and the background and the modulation are associated to environmental conditions, as illumination setup or object reflectance, for example.

In recent times, several methods have been developed for the phase demodulation from a single fringe pattern as given by Eq. (1) [1–3]. Although, originally, these methods were developed for the demodulation of 2D fringe patterns, the extension to an *n*-dimensional case is possible in the algorithms proposed by Servin et al. [1] and Marroquin et al. [2]. Very recently, Servin et al. [4] have proposed a generalization of the work of Larkin et al. [3] presenting a general *n*-dimensional quadrature transform. In all these methods background and modulation variations are considered as a source of phase estimation errors, which must be filtered before starting the demodulation process. This

* Corresponding author. Tel.: +34913944555; fax: +34913944678.
E-mail address: aq@fis.ucm.es (J. Antonio Quiroga).
[1] On sabatical leave at Centro de Investigaciones en Matemáticas A. C., Guanajuato 36000, Gto, Mexico.

0030-4018/$ - see front matter © 2003 Published by Elsevier B.V.
doi:10.1016/j.optcom.2003.07.014

process of background suppression and modulation normalization is denominated fringe pattern normalization. That is, the objective of a fringe pattern normalization method is to obtain, from a general signal given by Eq. (1), its normalized version given by

$$I_N(\mathbf{r}) = \cos\phi(\mathbf{r}), \tag{2}$$

where the modulation is set arbitrarily to a constant value of 1. Normalization methods can be useful also in another fringe processing technique as temporal phase sampling methods with temporal variation of background and/or modulation and fringe skeletonizing.

There exist several methods in the literature for fringe pattern normalization [5–9]. Envelope detection [5] and homomorphic processing of modulation [6] need to have a good model of the spatial distribution for both background, $b(\mathbf{r})$, and modulation, $m(\mathbf{r})$ (for example, the illumination produced by an expanded laser beam can be modeled as Gaussian), thus for a general case it is complex to apply them. Local histogram modification [7] and the modified regularized phase tracker for non-normalized fringe patterns [8] are non-linear methods for which the output depends strongly on the fringe-pattern's spatial structure, making them to be far from being direct techniques. The application of 2D Schlieren filtering [9] is a direct method but it suffers of spatial anisotropy in the resulting normalized fringe pattern due to the frequency structure of the corresponding filters. Finally, all the mentioned methods are difficult to extend to a general n-dimensional fringe pattern. In this work, we propose a fringe pattern normalization method that overcomes the mentioned drawbacks: it is direct, isotropic and automatically applicable to a general n-dimensional fringe pattern.

This work is organized as follows: in the following section we present the theoretical foundations of the method. In this section a brief introduction to the n-dimensional quadrature transform of Servin et al. [4] is made in order to clarify the role of the fringe orientation in the normalization method presented in this work, in particular we will show that the computation of the fringe orientation is not necessary for the normalization process, making possible a direct and computationally simple implementation of the proposed method. In Section 3, we test the normalization algorithm with a simulated and a real fringe pattern and finally conclusions are given in Section 4.

2. Theoretical foundations

2.1. The general n-dimensional quadrature transform

Given that the proposed normalization method is derived from the n-dimensional quadrature transform proposed in [4], we briefly review the theory behind this n-dimensional quadrature transform.

The aim of any n-dimensional quadrature operator $Q_n\{\cdot\}$ is to transform a given pattern into its quadrature. If we assume that the background is a spatially smooth function we can remove it by using a high-pass filter. If we denote by I_{HP} the high-pass filtered background-suppressed version of the irradiance signal given by Eq. (1), then

$$I_{\mathrm{HP}}(\mathbf{r}) = m(\mathbf{r})\cos\phi(\mathbf{r}) \tag{3}$$

and

$$Q_n\{I_{\mathrm{HP}}(\mathbf{r})\} = -m(\mathbf{r})\sin\phi(\mathbf{r}). \tag{4}$$

With this quadrature signal one can easily determine the phase $\phi(\mathbf{r})$ over the whole region of interest.

Knowing that in most practical situations the modulation $m(\mathbf{r})$ is a low frequency signal the gradient of I_{HP} can be well approximated by

$$\nabla I_{\mathrm{HP}}(\mathbf{r}) = -m(\mathbf{r})\sin[\phi(\mathbf{r})]\nabla\phi(\mathbf{r}), \tag{5}$$

if we multiply both sides of Eq. (5) by $\nabla\phi(\mathbf{r})$ and rearrange terms, we obtain the next expression for the quadrature operator

$$\begin{aligned} Q_n\{I_{\mathrm{HP}}(\mathbf{r})\} &= \frac{\nabla\phi(\mathbf{r})}{|\nabla\phi(\mathbf{r})|}\cdot\frac{\nabla I_{\mathrm{HP}}(\mathbf{r})}{|\nabla\phi(\mathbf{r})|} \\ &= \mathbf{n}_\phi(\mathbf{r})\cdot\frac{\nabla I_{\mathrm{HP}}(\mathbf{r})}{|\nabla\phi(\mathbf{r})|} \\ &= -m(\mathbf{r})\sin[\phi(\mathbf{r})] \end{aligned} \tag{6}$$

(note the vectorial character of the irradiance's gradient, thus the product by $\mathbf{n}_\phi$ is a dot product

between two vector fields). From (6) it is possible to see that the quadrature operator is composed of two terms, an orientation term $\mathbf{n}_\phi$ and a vector field $\mathbf{H}_n\{I_{\mathrm{HP}}\} = \nabla I_{\mathrm{HP}}/|\nabla\phi|$, we will proceed now to clarify their meaning.

The second term $\mathbf{H}_n\{I_{\mathrm{HP}}\} = \nabla I_{\mathrm{HP}}/|\nabla\phi|$ is a non-linear operator that can be interpreted as the n-dimensional generalization of the 1D Hilbert operator [4]. To our knowledge there exist two main ways to compute this field. The first way consists in the estimation of $|\nabla\phi|$ and further calculation of $\mathbf{H}_n\{\}$. This operation can be carried out with several techniques as, for example, the regularized method of Marroquin et al. [10] or the multichannel Gabor filter technique of Asundi and Jun [11]. The other possibility is to approximate the frequency response of $\mathbf{H}_n\{\}$ by n 1D Reisz filters along each spectral coordinate [3,4]. In effect, if we consider the fringe pattern as piecewise monochromatic, and a given filter with frequency response $H(\mathbf{q})$, where $\mathbf{q} = (u_1, \ldots, u_n)$ is the position vector in the spectral domain, we can use the next approximation [4]

$$\mathrm{FT}^{-1}\{H(\mathbf{q})\mathrm{FT}\{I(\mathbf{r})\}\} \approx H(\boldsymbol{\omega}(\mathbf{r}))I(\mathbf{r}), \tag{7}$$

that can be rewritten as

$$H(\mathbf{q})\mathrm{FT}\{I(\mathbf{r})\} \approx \mathrm{FT}\{H(\boldsymbol{\omega}(\mathbf{r}))I(\mathbf{r})\}, \tag{8}$$

where $\boldsymbol{\omega}(\mathbf{r}) = (\omega_1(\mathbf{r}), \ldots, \omega_n(\mathbf{r}))$ are the local spatial frequencies. From (8), we can write

$$\begin{aligned}\mathbf{H}_n\{I_{\mathrm{HP}}\} &= \frac{\nabla I_{\mathrm{HP}}}{|\nabla\phi|} = \mathrm{FT}^{-1}\left\{\mathrm{FT}\left\{\frac{\nabla I_{\mathrm{HP}}}{|\boldsymbol{\omega}(\mathbf{r})|}\right\}\right\} \\ &\approx \mathrm{FT}^{-1}\left\{\frac{1}{|\mathbf{q}|}\mathrm{FT}\{\nabla I_{\mathrm{HP}}\}\right\} \\ &= \mathrm{FT}^{-1}\left\{-\mathrm{i}\frac{\mathbf{q}}{|\mathbf{q}|}\mathrm{FT}\{I_{\mathrm{HP}}\}\right\},\end{aligned} \tag{9}$$

that is, $\mathbf{H}_n\{\cdot\}$ can be computed as

$$\mathbf{H}_n\{I_{\mathrm{HP}}(\mathbf{r})\} = \mathrm{FT}^{-1}\left\{-\mathrm{i}\frac{\mathbf{q}}{|\mathbf{q}|}\mathrm{FT}\{I_{\mathrm{HP}}(\mathbf{r})\}\right\}. \tag{10}$$

Eq. (10) states that the frequency response of $\mathbf{H}_n\{\cdot\}$ can be estimated by n 1D Reisz filters along each spectral coordinate, under the approximations explained above. This result was first obtained heuristically in 2D by Larkin et al. [3] and generalized, as presented, by Servin et al. [4]. From (10) it can be seen that the implementation of $\mathbf{H}_n\{\cdot\}$ with Reisz filters is an isotropic (there is only one singularity at the origin) generalization to n dimensions of the 1D Hilbert transform, and has the advantage that can be computed by fast Fourier transform methods, for these reasons in this work we will adopt this solution for the computation of $\mathbf{H}_n\{\cdot\}$.

The first term of Eq. (6) $\mathbf{n}_\phi(\mathbf{r}) = \nabla\phi(\mathbf{r})/|\nabla\phi(\mathbf{r})|$ is a unit vector normal to the corresponding isophasic contours, which points in the direction of $\nabla\phi(\mathbf{r})$. For example, in 2D, this vector points in the direction of the modulo 2π fringe orientation angle $\theta^{(2\pi)}$ [12], which is given by $\tan[\theta^{(2\pi)}] = \partial\phi/\partial y/\partial\phi/\partial x$. In n-dimensions, it is worth to express $\mathbf{n}_\phi$ in function of its direction cosines

$$\mathbf{n}_\phi(\mathbf{r}) = \frac{\nabla\phi(\mathbf{r})}{|\nabla\phi(\mathbf{r})|} = \sum_{k=1}^{n} c_k^{(2\pi)}\mathbf{e}_k, \tag{11}$$

where $\mathbf{e}_k, k = 1, \ldots, n$ is a orthonormal base in the direct space and $c_k^{(2\pi)}$ are the direction cosines given by

$$c_k^{(2\pi)} = \cos\alpha_k^{(2\pi)} = \frac{\partial\phi/\partial x_k}{|\nabla\phi(\mathbf{r})|}, \tag{12}$$

where $\alpha_k^{(2\pi)}, k = 1, \ldots, n$ are the modulo 2π orientation angles.

Unfortunately, there is no direct way (e.g., a linear transformation) to obtain $\mathbf{n}_\phi$ from a single-image fringe pattern with closed fringes. And this is the reason of the fundamental ambiguity in the global sign of the demodulated phase by using the quadrature operator $Q_n\{\cdot\}$.

2.2. Fringe pattern normalization by the n-dimensional quasi-quadrature transform

As mentioned above, it is not possible to find a linear system to calculate the orientation field $\mathbf{n}_\phi$ for an image with closed fringes. The reason is that the phase ϕ is wrapped by the observation process, so we do not have access to it (otherwise the problem of phase demodulation and normalization would be solved). To obtain the orientation field we have only access to the irradiance image and its gradient. Let us compute a new set of direction cosines computed from the irradiance's gradient instead of the phase's gradient:

$$c_k = \cos\alpha_k = \frac{\partial I/\partial x_k}{|\nabla I(\mathbf{r})|}. \tag{13}$$

If we assume, as before, that the modulation $m(\mathbf{r})$ and the background $b(\mathbf{r})$ are spatially smooth, Eq. (13) becomes

$$c_k = \frac{\sin\phi}{|\sin\phi|}\frac{\partial\phi/\partial x_k}{|\nabla\phi|} = \operatorname{sign}[\sin\phi]\frac{\partial\phi/\partial x_k}{|\nabla\phi|}, \tag{14}$$

and according to Eq. (12)

$$c_k = \operatorname{sign}[\sin\phi]c_k^{(2\pi)}. \tag{15}$$

Then, if we compute the orientation field from the irradiance's gradient, we obtain

$$\tilde{\mathbf{n}}_\phi(\mathbf{r}) = \frac{\nabla I}{|\nabla I|} = \sum_{k=1}^{n} c_k\mathbf{e}_k = \operatorname{sign}[\sin\phi]\mathbf{n}_\phi(\mathbf{r}). \tag{16}$$

From Eq. (16) we see that $\tilde{\mathbf{n}}_\phi$ and $\mathbf{n}_\phi$ have the same orientation but opposite direction every time the $\sin\phi$ changes its sign. Due to this sign change, using $\tilde{\mathbf{n}}_\phi$ instead of $\mathbf{n}_\phi$ gives place to a new operator, we have called quasi-quadrature operator,

$$\widetilde{\mathcal{Q}}_n\{I_{\mathrm{HP}}\} = \tilde{\mathbf{n}}(\mathbf{r})\cdot\mathbf{H}_n\{I_{\mathrm{HP}}\} \tag{17}$$

that using Eq. (16) is given by

$$\widetilde{\mathcal{Q}}_n\{I_{\mathrm{HP}}(\mathbf{r})\} = -\operatorname{sign}[\sin\phi]m(\mathbf{r})\sin\phi(\mathbf{r}). \tag{18}$$

Finally, if we compute the modulating phase using this quasi-quadrature term we obtain

$$\begin{aligned} W\{\tilde{\phi}\} &= \arctan\left(\frac{-\widetilde{\mathcal{Q}}_n\{I_{\mathrm{HP}}\}}{I_{\mathrm{HP}}}\right) \\ &= \operatorname{sign}[\sin\phi]W\{\phi\}, \end{aligned} \tag{19}$$

where $W\{\cdot\}$ denotes the wrapping operator [13].

From Eq. (19) we see that the phase maps $W\{\tilde{\phi}\}$ and $W\{\phi\}$ only differ in sign every time $\sin\phi$ changes its sign. In consequence from $W\{\tilde{\phi}\}$ we can compute the normalized version of $I(\mathbf{r})$ as

$$I_N(\mathbf{r}) = \cos[W\{\tilde{\phi}(\mathbf{r})\}] = \cos\phi(\mathbf{r}). \tag{20}$$

From a practical point of view the computation of the orientation field $\tilde{\mathbf{n}}\phi$ is not necessary for the normalization, from (13) and (17) the quasi-quadrature operator is given by

$$\widetilde{\mathcal{Q}}_n\{I\} = \frac{\nabla I}{|\nabla I|}\cdot\frac{\nabla I}{|\nabla\phi|} = \frac{|\nabla I|}{|\nabla\phi|}, \tag{21}$$

then, finally the general expression used to compute the quasi-quadrature operator is

$$\widetilde{\mathcal{Q}}_n\{I_{\mathrm{HP}}\} = |\mathbf{H}_n\{I_{\mathrm{HP}}\}|, \tag{22}$$

where as before $\mathbf{H}_n\{\,\}$ is the n-dimensional Hilbert operator used. Eq. (22) states that the quasi-quadrature operator does not depend on the orientation; in consequence the normalized fringe pattern has no error related with the orientation term. The only error remaining is the one that comes from the approximation used for the computation of the Hilbert operator $\mathbf{H}_n\{I_{\mathrm{HP}}\} = \nabla I_{\mathrm{HP}}/|\nabla\phi|$. For example, in the normalization technique presented in [9] $\mathbf{H}_n\{\,\}$ was implemented as a 2D Schlieren filter, making necessary the use of two orthogonal directions to compensate for the poor response of the Schlieren filter along the spectral discontinuity.

The solution proposed is direct (two linear operators consisting in the high-pass filter to generate I_{HP} and the Reisz filter implementation for the Hilbert operator $\mathbf{H}_n\{\cdot\}$ given by Eq. (10)) and isotropic (given that the high-pass filter used is also isotropic, for example, a circular top hat). Finally, the normalization method proposed is automatically applicable in any n-dimensional case.

Another interesting point of the proposed method is that we can compute a reliability map of the recovered normalized fringe pattern. This quality map can be estimated from the modulation associated to the phase map $W\{\tilde{\phi}\}$ (Eq. (19)) that is given by

$$m_N = \sqrt{I_{\mathrm{HP}}^2 + \left(\widetilde{\mathcal{Q}}_n\{I_{\mathrm{HP}}\}\right)^2}, \tag{23}$$

This field includes both the modulation of the original fringe pattern as well as the frequency response of the filter used to implement the quasi-quadrature filter $\widetilde{\mathcal{Q}}_n\{\cdot\}$ (in our case the response corresponding to the Reisz filters used to compute $\mathbf{H}_n\{\cdot\}$). As the quasi-quadrature filter $\widetilde{\mathcal{Q}}_n\{\cdot\}$ does not depend on the orientation field the modulation m_N has no errors related with it. The modulation computed by Eq. (23) can be used to segment the normalized fringe pattern, making possible the automatic definition of the region of interest, which could be used by a demodulation algorithm. Eq. (23) is an n-dimensional formula to obtain the modulation of a high-pass filtered fringe pattern

that coincides in the 2D case with the amplitude demodulation technique presented in [3], when the operator $\widetilde{Q}_n\{\cdot\}$ is implemented with Reisz filters.

It is worth mentioning that the proposed normalization technique is equivalent to a modulation division (as it should be). From (19) and (20), we can write

$$I_N = \cos\phi = \frac{I_{\mathrm{HP}}}{\sqrt{I_{\mathrm{HP}}^2 + \left(\widetilde{Q}_n\{I_{\mathrm{HP}}\}\right)^2}} = \frac{I_{\mathrm{HP}}}{m_N}. \tag{24}$$

Eq. (24) states that the $\cos(\arctan(-\widetilde{Q}_n\{I_{\mathrm{HP}}\}/I_{\mathrm{HP}}))$ method is equivalent to estimate the modulation m_N and normalize I_{HP} with respect to it. Although mathematically equivalent, there are computational differences between the proposed normalization method and the modulation division. The first difference is the possible division by zero that can happen in the modulation division being in this case automatically managed by the atan2(·) C/C++ function. The second is that the proposed technique guarantees normalization between −1 and 1 through the $\cos(W\{\widetilde{\phi}\})$ computation, this being very useful in several phase demodulation techniques.

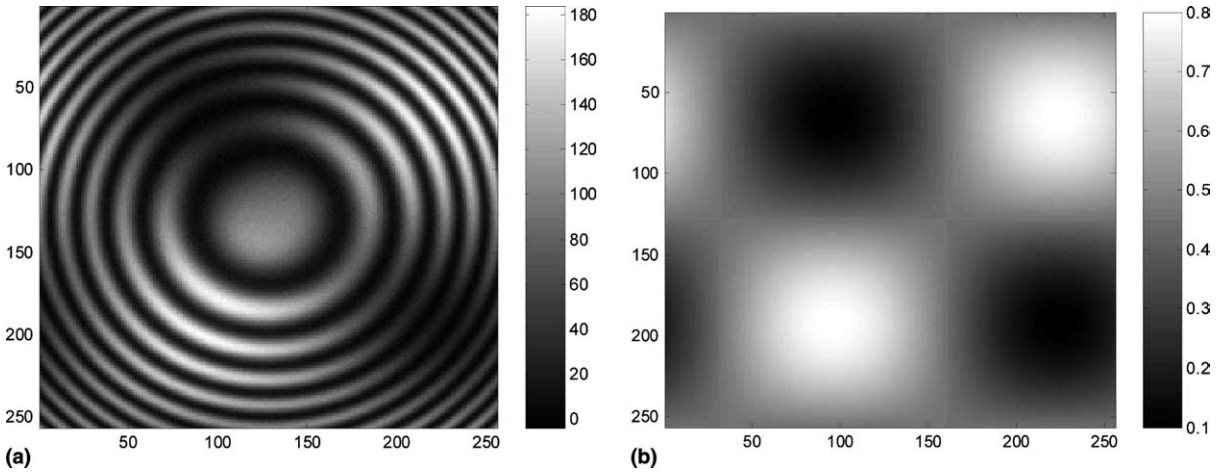

Fig. 1. (a) Simulated fringe pattern with spatially varying background and modulation. (b) Modulation $m(\mathbf{r})$ of the fringe pattern of (a).

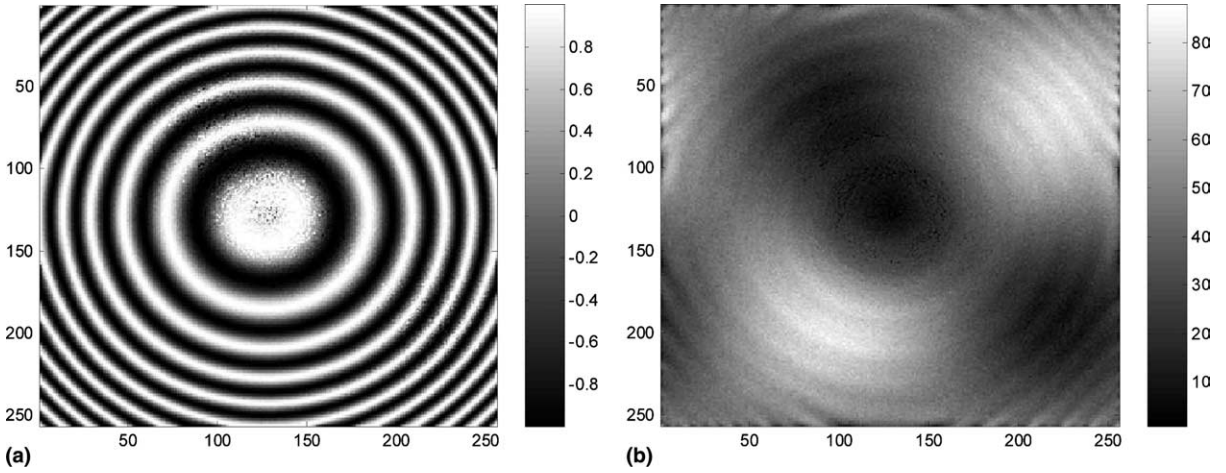

Fig. 2. (a) Normalized image, corresponding to Fig. 1(a), obtained by the proposed method. (b) Quality map obtained for the normalized image shown in (a). Dark and bright areas correspond to low and high values, respectively.

3. Experimental results

For the examples shown in this section we have computed the Hilbert operator $\mathbf{H}_n\{\cdot\}$ given by Eq. (10). As high pass filter we have used a cosenoidal shaped filter with cut-off frequency of 5 fringes/field.

The first example is a computer generated fringe pattern given by

$$I(x,y) = \text{round}[128 \cdot m(x,y) + 100 \cdot m(x,y) \times \cos[40\pi(x^2+y^2)/N^2] + f(x,y)], \qquad (25)$$

where $N = 256$, $x,y = -N/2,\ldots,N/2-1$, f is a zero mean, Gaussian distributed signal with a standard deviation of 2, modeling additive electronic noise, m is a 2D sinusoidal image representing the modulation of the fringe pattern with minimum value 0.1 and maximum value 0.8, and round$[\cdot]$ indicates the rounding to the nearest integer operation. In this case, the modulation m has a spatial frequency of 1 fringe/field in both directions and the fringe pattern has a spatial frequency content that covers the range from 0 to 20 fringes/field (in the x and y axes), thus there exists some spectral overlapping between m and I. Fig. 1(a) shows the 256×256 simulated fringe pattern generated by Eq. (25), the used modulation m is

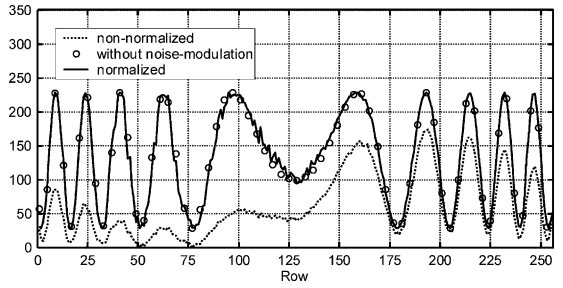

Fig. 3. Profile along column 80 for the non-normalized fringe pattern of Fig. 1(a) (dot line), the normalized fringe pattern shown in Fig. 2(a) (continuous line) and the theoretical fringe pattern without background and normalized modulation (open circles).

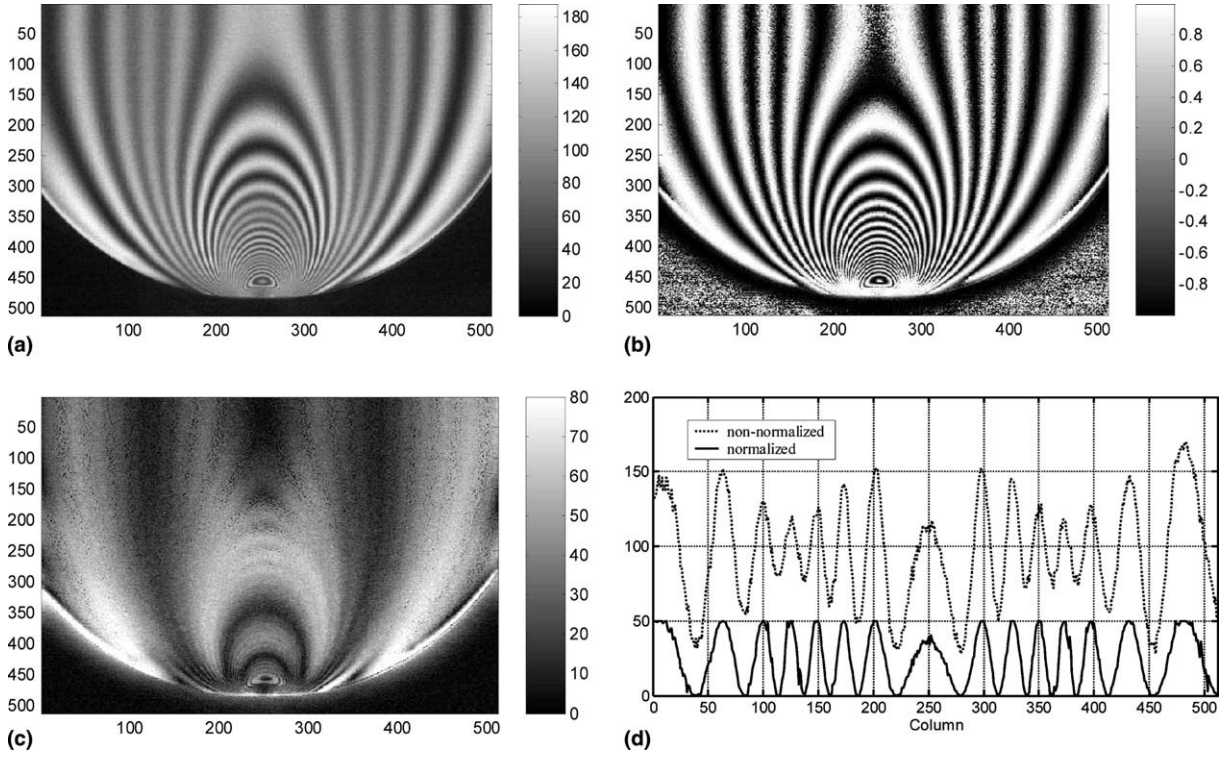

Fig. 4. (a) B-band of a RGB isochromatic fringe pattern corresponding to a diametrally compressed disk. (b) Normalized fringe pattern computed from (a). (c) Quality map obtained from the normalization process for (b). (d) Profile along line 250 for the non-normalized isochromatic fringe pattern of (a) (dot line) and the normalized image of (b) (continuous line).

shown in Fig. 1(b). Fig. 2(a) shows the normalized fringe computed by Eq. (20) and Fig. 2(b) the reliability map computed by (23) (note the scaling factor of 100 in Eq. (25)). In Fig. 2(b) it can be observed that the quality map reflects the combined effects of the modulation of the original fringe pattern and the frequency response of the n-dimensional quasi-quadrature operator, this behavior is especially visible in the central part of the fringe pattern where the local spatial frequency is close to zero. Fig. 3 shows a comparison of the profiles along column 80 of the original irradiance, the normalized irradiance and the original simulated irradiance without noise-modulation.

The second example is an experimental isochromatic fringe pattern obtained in a photoelastic experiment. The sample is a diametrally compressed disk, observed in the transmission mode in the circular dark field configuration of a circular polariscope [14]. Fig. 4(a) shows a 512×512 image corresponding to the B band of an RGB image captured with a 3 chip RGB-CCD, due to the illuminant's spectrum the B band of the isochromatic pattern shows a periodic lack of modulation clearly visible in Fig. 4, this effect is specially remarkable in the zone near the contact point where the highest spatial frequencies are present. Figs. 4(b) and (c) show the normalized fringe pattern and the quality map obtained by our method, respectively (note that the quality map is not normalized as in the former example). Fig. 4(c) shows again the effects of the modulation bands corresponding to the isochromatic fringe pattern and the response of the quasi-quadrature filter. Finally, Fig. 4(d) shows a comparison of the profiles along row 250 for the non-normalized and the normalized fringe patterns of Figs. 4(a) and (b).

4. Conclusions

We have presented a new fringe n-dimensional fringe pattern normalization algorithm based in the use of the so-called n-dimensional quasi-quadrature transform. The method is direct and also due to the properties of the *n-dimensional* Hilbert operator used the proposed method is isotropic. We have tested the algorithm with real data obtaining good results.

Acknowledgements

The authors thank the reviewer for his opportune and useful comments. We thank the economical support of this work given by project DPI2002-02104 of the Ministerio de Ciencia y Tecnología of Spain and to the Consejo Nacional de Ciencia y Tecnologia of Mexico.

References

[1] M. Servin, J.L. Marroquin, F.J. Cuevas, J. Opt. Soc. Am. A 18 (2001) 689.
[2] J.L. Marroquin, R. Rodriguez-Vera, M. Servin, J. Opt. Soc. Am. A 15 (1998) 1536.
[3] K.G. Larkin, D.J. Bone, M.A. Oldfield, J. Opt. Soc. Am. A 18 (2001) 1862.
[4] M. Servin, J.A. Quiroga, J.L. Marroquin, J. Opt. Soc. Am. 20 (2003) 925.
[5] Q. Yu, K. Andersen, W. Osten, W. Jüptner, Appl. Opt. 20 (1996) 3783.
[6] T. Kreis, Holographic Interferometry, Akademie Verlag, Berlin, 1996.
[7] S. de Nicola, P. Ferraro, I. Gurov, R. Koviazin, M. Volkov, Meas. Sci. Tech. 11 (2000) 1328.
[8] R. Legarda-Saénz, W. Osten, W. Jüptner, Appl. Opt. 41 (2002) 5519.
[9] J.A. Quiroga, J.A. Gomez Pedrero, A. Garcia Botella, Opt. Commun. 197 (2001) 43.
[10] J.L. Marroquin, R. Rodriguez-Vera, M. Servin, J. Opt. Soc. Am. A 15 (1998) 1536.
[11] A. Asundi, W. Jun, Opt. Eng. 41 (2002) 1400.
[12] J.A. Quiroga, M. Servin, F.J. Cuevas, J. Opt. Soc. Am. A 19 (2002) 1524.
[13] D. Ghiglia, M.D. Pritt, Two-dimensional Phase Unwrapping, John Wiley, New York, 1998.
[14] P.S. Teocaris, E.E. Gdoutos, Matrix Theory of Photoelasticity, Springer-Verlag, Berlin, 1979.